

Recombinant Klotho protein protects pulmonary alveolar epithelial cells against sepsis-induced apoptosis by inhibiting the Bcl-2/Bax/caspase-3 pathway

Xiao Bo Li^{1,2,A–C,E,F}, Jia Li Liu^{1,2,B,C}, Shuang Zhao^{1,2,C}, Jing Li^{1,2,B,D}, Guang-Yan Zhang^{1,2,C,D}, Qing Tang^{1,2,B}, Wei Yong Chen^{1,2,A,C}

¹ Respiratory Department, Chengdu Seventh People's Hospital, China

² Respiratory Department, Tumor Hospital Affiliated to Chengdu Medical College, China

A – research concept and design; B – collection and/or assembly of data; C – data analysis and interpretation;

D – writing the article; E – critical revision of the article; F – final approval of the article

Advances in Clinical and Experimental Medicine, ISSN 1899–5276 (print), ISSN 2451–2680 (online)

Adv Clin Exp Med. 2025;34(1):123–134

Address for correspondence

Xiao Bo Li

E-mail: xiaoboli2023@163.com

Funding sources

This study was supported by the Joint Foundation of Chengdu Medical College and Chengdu Seventh People's Hospital (grant No. 2020LHJYPJ-05).

Conflict of interest

None declared

Acknowledgements

We would like to thank the Molecular Biological Center of Chongqing Medical University for providing us with laboratory and equipment.

Received on March 20, 2023

Reviewed on July 17, 2023

Accepted on February 20, 2024

Published online on May 14, 2024

Cite as

Li XB, Liu JL, Zhao S. Recombinant Klotho protein protects pulmonary alveolar epithelial cells against sepsis-induced apoptosis by inhibiting the Bcl-2/Bax/caspase-3 pathway. *Adv Clin Exp Med.* 2025;34(1):123–134. doi:10.17219/acem/184639

DOI

10.17219/acem/184639

Copyright

Copyright by Author(s)

This is an article distributed under the terms of the Creative Commons Attribution 3.0 Unported (CC BY 3.0) (<https://creativecommons.org/licenses/by/3.0/>)

Abstract

Background. Inflammation-induced apoptosis of alveolar type II epithelial cells is a primary contributor to sepsis-induced acute respiratory distress syndrome (ARDS). Klotho is a single-pass transmembrane protein with anti-inflammatory and anti-apoptotic effects. However, the role and mechanism of Klotho in the development of ARDS remains unknown.

Objectives. This study aimed to investigate the effect of Klotho on sepsis-induced apoptosis in human pulmonary alveolar epithelial cells (HPAEPiCs) together with the potential mechanism.

Materials and methods. Cecal ligation and puncture (CLP) were performed to generate an in vivo sepsis model, and HPAEPiCs were treated with lipopolysaccharide (LPS) to mimic sepsis in vitro. Both models were administered recombinant Klotho protein. The morphology of the lung tissue was observed, and apoptotic cells and cell viability were detected. Interleukin (IL)-1 β , IL-6, and tumor necrosis factor alpha (TNF- α) levels were detected using enzyme-linked immunosorbent assay (ELISA), while the expression of Bcl-2, Bax and cleaved caspase-3 was detected with western blotting.

Results. Klotho reversed the CLP-induced decrease in mouse survival in vivo ($p < 0.001$) and increased inflammatory cell infiltration and inflammatory substance exudation in the lung tissue of mice with sepsis (both $p < 0.001$). Klotho also suppressed apoptosis ($p < 0.001$) as demonstrated by IL-1 β , IL-6 and TNF- α expression (all $p < 0.001$), and Bcl-2/Bax/caspase-3 pathway activation ($p < 0.001$). Klotho pretreatment significantly prevented LPS-induced apoptosis in vitro ($p < 0.001$), as demonstrated by IL-1 β , IL-6 and TNF- α upregulation (all $p < 0.001$); and Bcl-2/Bax/caspase-3 pathway activation in HPAEPiCs ($p < 0.001$).

Conclusions. This study demonstrated that Klotho can ameliorate acute lung injury (ALI) induced by sepsis by inhibiting inflammatory responses and exerting anti-apoptotic effects by suppressing Bcl-2/Bax/caspase-3 pathway activation.

Key words: sepsis, ARDS, apoptosis, Klotho, HPAEPiC

Background

Sepsis is a life-threatening inflammatory response, with approx. 30% mortality rate.¹ The lungs are the most vulnerable organ attacked by inflammatory factors during sepsis, and sepsis progresses to acute respiratory distress syndrome (ARDS) in approx. 50% of patients.² Although great progress has been made recently in the treatment of ARDS, its morbidity and mortality remain high.³ Therefore, understanding the complex pathogenesis of ARDS is of great significance. Acute respiratory distress syndrome is a complex clinical syndrome with a heterogeneous clinical phenotype, and it is characterized by pulmonary edema in the interstitium and air spaces of the lungs. The accumulation of fluid increases the work of breathing and impairs gas exchange, resulting in hypoxemia, reduced CO₂ excretion and, ultimately, acute respiratory failure.⁴ Acute respiratory failure ultimately leads to hypoxia, which has a poor prognosis.^{5,6} Furthermore, acute respiratory failure is among the sequela of complications that can develop in response to sepsis, which can induce severe inflammatory responses.⁷

Sepsis is facilitated by bacterial infections inducing the excessive release of inflammatory cytokines, such as tumor necrosis factor alpha (TNF- α), interleukin (IL)-1 and IL-6, causing cellular injury and multiple organ dysfunction syndrome.⁸ Lipopolysaccharide (LPS) is a bacterial endotoxin that can induce a severe inflammatory response.⁹ Lipopolysaccharide is commonly used to establish murine lung injury models to mimic sepsis-induced ARDS in humans, and such models help investigate the pathogenesis of ARDS.¹⁰ Alveolar epithelial cell apoptosis complicates the pathogenesis of ARDS.¹¹ Apoptosis can be activated by 2 pathways, namely, the mitochondrial pathway and the external death receptor pathway. When cells encounter direct or indirect DNA damage, reactive oxygen species (ROS), hypoxia, or inflammation, the mitochondrial apoptosis pathway is activated.^{12,13} These stimuli ultimately disrupt mitochondrial function by inducing the expression of proapoptotic Bcl-2 family members, such as Bcl-2, Bax and Bak.¹⁴ The imbalance of Bax and Bcl-2 can induce the activation of caspase-3,¹⁵ thereby promoting apoptosis.¹⁶ Many studies have revealed that LPS induces apoptosis in HPAEpiCs.^{17,18} However, the mechanism of LPS-induced HPAEpiCs apoptosis has not yet fully elucidated.

It has been reported that acute inflammation/sepsis suppresses the activation of α -Klotho, and α -Klotho upregulation during acute sepsis may participate in the counter-regulatory response to severe inflammation in patients with sepsis.¹⁹ Klotho deficiency aggravates sepsis-related multiple organ dysfunction.²⁰ Klotho has been recognized as a gene involved in the aging process in mammals for more than 30 years,²¹ and this single-pass transmembrane protein counteracts oxidative stress²² and cell senescence²³ and promotes autophagy.²⁴ In addition, Klotho has anti-apoptotic effects.²⁵ Klotho suppresses diabetes-induced

podocyte apoptosis²⁶ and inhibits H₂O₂-induced apoptosis in periodontal ligament stem cells.²⁷ Normal lungs do not express Klotho protein, but they can obtain cell protection from soluble circulating Klotho.²⁸ However, the effect of Klotho on sepsis-induced apoptosis in alveolar epithelial cells has not been reported. Chen et al. revealed that Klotho can inhibit proliferation and increase apoptosis in A549 cells by regulating the expression of the apoptosis-related genes Bcl-2 and Bax.²⁹ Therefore, we hypothesized that Klotho protects alveolar epithelial cells against sepsis or LPS-induced apoptosis by inhibiting the Bcl-2/Bax/caspase-3 pathway.

Objectives

The objective of this study was to explore the effects of Klotho on sepsis-induced inflammatory cytokine release and LPS-induced HPAEpiC apoptosis and demonstrate the potential mechanism of Klotho protects HPAEpiC against sepsis or LPS-induced apoptosis.

Materials and methods

Cecal ligation and puncture (CLP) were performed to generate a mouse sepsis model, and HPAEpiCs were treated with LPS to create an in vitro model of sepsis-induced ARDS. Both models were treated with recombinant Klotho protein to explore its effects on sepsis-induced alveolar type II epithelial cells and its potential mechanism.

Cell culture

The HPAEpiC was brought from the American Type Culture Collection (ATCC, Manassas, USA). The cells were cultured in a high glucose Dulbecco's modified Eagle's medium (DMEM) containing 10% fetal bovine serum (FBS) and incubated at 37°C under 5% CO₂ and 95% humidity; then, cells were passaged when confluence reached 90%. The use of HPAEpiC was approved by the Human Ethics Committee of Chengdu Seventh People's Hospital on January 26, 2022 (Human Experimental Inspection Form of Chengdu Seventh People's Hospital No. 2200647).

Animals and treatment

The C57BL/6 mice (male, 8 weeks old, weight = 20–25 g) were purchased from ENSIWEIER Biotechnology Co., LTD (Chongqing, China). The mice were supplied sterile water and food and kept in a specific pathogen-free environment (temperature: 22°C \pm 2°C; humidity: 40–60%). The animal experiment was approved by the Animal Ethics Committee of Chengdu Seventh People's Hospital on January 13, 2022 (Animal Experimental Ethical

Inspection Form of Chengdu Seventh People's Hospital No. 2200638). The mice were randomly divided into 4 groups, namely, the sham, Klotho, CLP, and CLP+Klotho groups ($n = 10/\text{group}$). Mice in the sham group underwent sham operation without CLP, whereas mice in the Klotho group were intraperitoneally injected with recombinant mouse Klotho protein (10 $\mu\text{g}/\text{kg}$; R&D Systems, Minneapolis, USA). Mice in the CLP group underwent CLP, and those in the CLP+Klotho group underwent CLP, followed by intraperitoneal treatment with recombinant mouse Klotho protein. Then, 24 h after CLP, 2% isoflurane was used to anesthetize the mice, which were euthanized via cervical dislocation, and their lungs were collected for hematoxylin and eosin (H&E) staining, terminal deoxynucleotidyl transferase-mediated biotinylated UTP labeling (TUNEL) assay and western blotting.

Cecal ligation and puncture mouse model

Cecal ligation and puncture mouse model was created as described previously.³⁰ In brief, after anesthesia was induced with 2% isoflurane, the cecum of each mouse was completely exposed through an abdominal surface incision. Then, 70% of the total length of the cecum was ligated with a 4-0 silk suture and a penetrating puncture was performed with a No. 22 needle (BD Biosciences, Franklin Lakes, USA). Sham-operated mice underwent the same procedure without ligation and puncture of the cecum.

Humane endpoints of surgery/treatment in mice

Several evaluation items are often used as the endpoints of animal experiments. First, experiments may cause pain and discomfort to animals. If drugs or other methods cannot be used to relieve their pain and distress, euthanasia is performed. Second, animals should be euthanized in response to the rapid weight loss of 15–20% or cachexia and long-term muscle catabolism. Third, animals should be euthanized if they do not eat for 24–48 h or if they ingest only a small amount of food for 3 days. Lastly, animals should be euthanized when they cannot drink or eat by themselves.

Survival studies

Survival rates were assessed as described by Alves et al.³¹ To evaluate the effect of Klotho on the survival of mice with sepsis, 80 mice were randomly divided into the sham, Klotho, CLP, and CLP+Klotho groups ($n = 20/\text{group}$). The mice in the CLP+Klotho and Klotho groups received intraperitoneal injections of 10 $\mu\text{g}/\text{kg}$ Klotho once daily. Survival curves were plotted every 6–12 h for 7 consecutive days. After 7 days, 2% isoflurane was used to anesthetize the surviving mice, which were euthanized via cervical dislocation.

Collection of bronchoalveolar lavage fluid and cell culture medium for IL-1 β , IL-6 and TNF- α detection

Bronchoalveolar lavage fluid (BALF) was collected as previously described.³² In brief, all mice were anesthetized with 2% isoflurane and immediately subjected to thoracotomy, and the right great bronchus below the tracheal bifurcation was ligated. Then, the left bronchial tube was intubated and rinsed 3 times with ice-cold phosphate-buffered saline (PBS) (0.5 mL). The mice were sacrificed via cervical dislocation under anesthesia. We also collected the culture medium of HPAEpiCs. In brief, the cells were treated with 0.1 mg/L, 1 mg/L or 10 mg/L LPS or 10 mg/L LPS combined with 50 mg/L recombinant Klotho for 24 h; then, the conditioned culture media was collected. The collected BALF and cell culture medium were centrifuged at $1000 \times g$ and 4°C for 10 min. The supernatant was stored at -80°C for further analysis. The total protein level was detected using the bicinchoninic acid (BCA) assay kit (Beyotime Biotechnology, Shanghai, China), and the protein concentration was standardized before enzyme-linked immunosorbent assay (ELISA) detection (Beyotime Biotechnology) of IL-1 β , IL-6 and TNF- α in BALF and cell culture medium according to the manufacturer's protocol.

Hematoxylin and eosin staining

Morphological changes in the lungs of mice were evaluated with H&E staining.³³ In brief, paraffin sections of lung tissue were soaked in xylene I and xylene II for 10 min. Then, the sections were successively incubated in 100% (I, II), 90%, 80%, and 70% alcohol for 5 min each and rinsed 3 times with running water for 5 min each. Finally, the sections were stained with hematoxylin for 5 min and eosin (1%) staining for 2 min, then rinsed with water. Images of the lung tissues were captured (magnification: $\times 400$) using an optical microscope (Leica DFC550 DM4 B; Leica Camera AG, Wetzlar, Germany).

TUNEL assay

To detect apoptosis in lung tissue in situ, we used a TUNEL kit.³⁴ In brief, 5- μm -thick paraffin sections of lung tissue were dewaxed, rehydrated, and treated with protease K working solution for 30 min. The slides were then incubated in the TUNEL reaction mixture at 37°C for 1 h. The slides were stained with 4',6-diamidino-2-phenylindole (DAPI) for 5 min, and the tissue was mounted in an Anti-Fade Mounting Medium. Images of the lung tissues were captured using an optical microscope (magnification $\times 200$; Leica DFC550 DM4 B).

Cell Counting Kit-8 cell viability assay

Changes in cell viability were determined using the Cell Counting Kit-8 (CCK-8) assay.³⁵ In brief, HPAEpiCs (5×10^3 /well) were plated in 96-well plates. The cells were exposed to LPS (0.1 mg/L, 1 mg/L or 10 mg/L) for 24 h or 10 mg/L LPS for 12 h, 24 h or 48 h. Then, 10 μ L of CCK-8 was added to each well. The absorption of each well was read at 450 nm using a microplate reader (Bio-Rad 680; Bio-Rad Hercules, USA). In addition, cells were pretreated with 10 mg/L LPS for 1 h and then incubated with various concentrations (0 mg/L, 50 mg/L and 100 mg/L) of recombinant Klotho protein for 24 h or 50 mg/L recombinant Klotho protein for 12 h, 24 h or 48 h. Cell Counting Kit-8 was added to each well as previously described, and the plate was incubated at 37°C for 1 h. The absorption of each well was read at 450 nm using a microplate reader (Bio-Rad 680; Bio-Rad).

Annexin/propidium iodide (PI) staining

Annexin V/propidium iodide (PI) staining was used to investigate cell apoptosis.³⁶ In brief, cells were exposed to 0.1 mg/L, 1 mg/L or 10 mg/L LPS or 10 mg/L LPS combined with 50 mg/L recombinant Klotho for 24 h. Untreated cells served as the control group. The cells were then harvested and washed with PBS to remove the medium. At least 1×10^5 cells were resuspended in 100 μ L of binding buffer containing Annexin V-FITC and PI and incubated for another 15 min at room temperature in the dark. Fluorescence from 1×10^4 cells in the Annexin V-FITC and PI binding channels FL-1 (Annexin V-FITC) and FL-3 (PI) was quantified using FACScan and analyzed using Cellquest Pro (BD Biosciences, Franklin Lakes, USA).

Western blotting

Protein expression was detected with western blotting as previously described.³⁷ The cells and lung tissue of mice were lysed using radioimmunoprecipitation assay (RIPA) lysis buffer containing protease and phosphatase inhibitors and centrifuged for 15 min at $12,700 \times g$ and 4°C. The supernatant was collected, the protein concentration was measured, and the samples were boiled for 5 min. Then, 30 μ g of protein was electrophoresed on an 8% sodium dodecyl sulfate-polyacrylamide gel electrophoresis (SDS-PAGE) gel, transferred to a polyvinylidene difluoride (PVDF) membrane, and blocked with 5% skim milk at room temperature for 2 h. The membrane was incubated overnight with primary antibodies against GAPDH (ab8245; 1:5000), Bcl-2 (ab182858; 1:1000), Bax (ab32503; 1:1000), pro-caspase-3 (ab32499; 1:1000), and cleaved caspase-3 (ab214430; ab2302; 1:1000; all from: Abcam, Cambridge, UK) at 4°C, then washed 3 times with Tris-buffered saline containing 0.1% Tween-20, then incubated with HRP Anti-Rabbit IgG antibody (ab288151; 1:10000; Abcam) for 2 h. The protein bands were visualized using

chemiluminescence and analyzed using Quantity One software v. 6.0 (Bio-Rad).

Statistical analyses

All experiments were repeated at least 3 times, and data were expressed as the mean \pm standard deviation ($M \pm SD$). All the data were analyzed using GraphPad Prism 8.0 (GraphPad Software, San Diego, USA). Statistical significance was indicated by $p < 0.05$. Quantitative data were presented as dots and medians. The survival analysis between groups used the log-rank (Mantel–Cox) method, and due to the limited sample size, other data were assessed with non-parametric tests. The Kruskal–Wallis test was used for a comparison of 3 or more groups, followed by Dunn's post hoc test. The medians and quartiles were presented in supplement tables. The test levels of $\alpha = 0.05$ and $p < 0.05$ were considered significant.

Results

Klotho increased mouse survival and decreased IL-1 β , IL-6 and TNF- α levels

To determine the effects of Klotho on mice with sepsis, mice that underwent CLP were intraperitoneally injected with recombinant Klotho protein. All mice in the CLP group died on day 4, whereas 40% of those in the CLP+Klotho group survived ($p < 0.002$, Fig. 1A). Hematoxylin and eosin staining of mouse lung tissue in the CLP group revealed swelling, cell edema, inflammatory cell infiltration, and inflammatory mediator exudation, and these effects were ameliorated by Klotho treatment (Fig. 1B). We also detected IL-1 β , IL-6 and TNF- α in the BALF of mice. The results showed that IL-1 β ($p < 0.001$), IL-6 ($p < 0.001$) and TNF- α ($p < 0.001$) levels were significantly higher in the CLP group compared to the sham group, and these increases were significantly reduced by Klotho treatment (all $p < 0.05$; Fig. 1C–E).

Effects of Klotho on alveolar epithelial cell apoptosis and Bcl-2/Bax/caspase-3 signaling in mice with sepsis

To detect the effect of Klotho on alveolar epithelial cell apoptosis in mice with sepsis, apoptotic cells were detected using TUNEL staining. The number of TUNEL-positive cells was significantly higher in the CLP group compared to sham mice ($p < 0.001$) and CLP+Klotho groups ($p < 0.05$; Fig. 2A,B). We also detected the protein levels of Bcl-2, Bax and caspase-3 in the lung tissue of mice, finding that CLP decreased the Bcl-2/GAPDH ratio ($p < 0.001$) and increased the Bax/GAPDH ($p < 0.001$) and cleaved caspase-3/caspase-3 ratios ($p < 0.001$); and these effects were reversed by Klotho treatment (all $p < 0.05$; Fig. 2C,D).

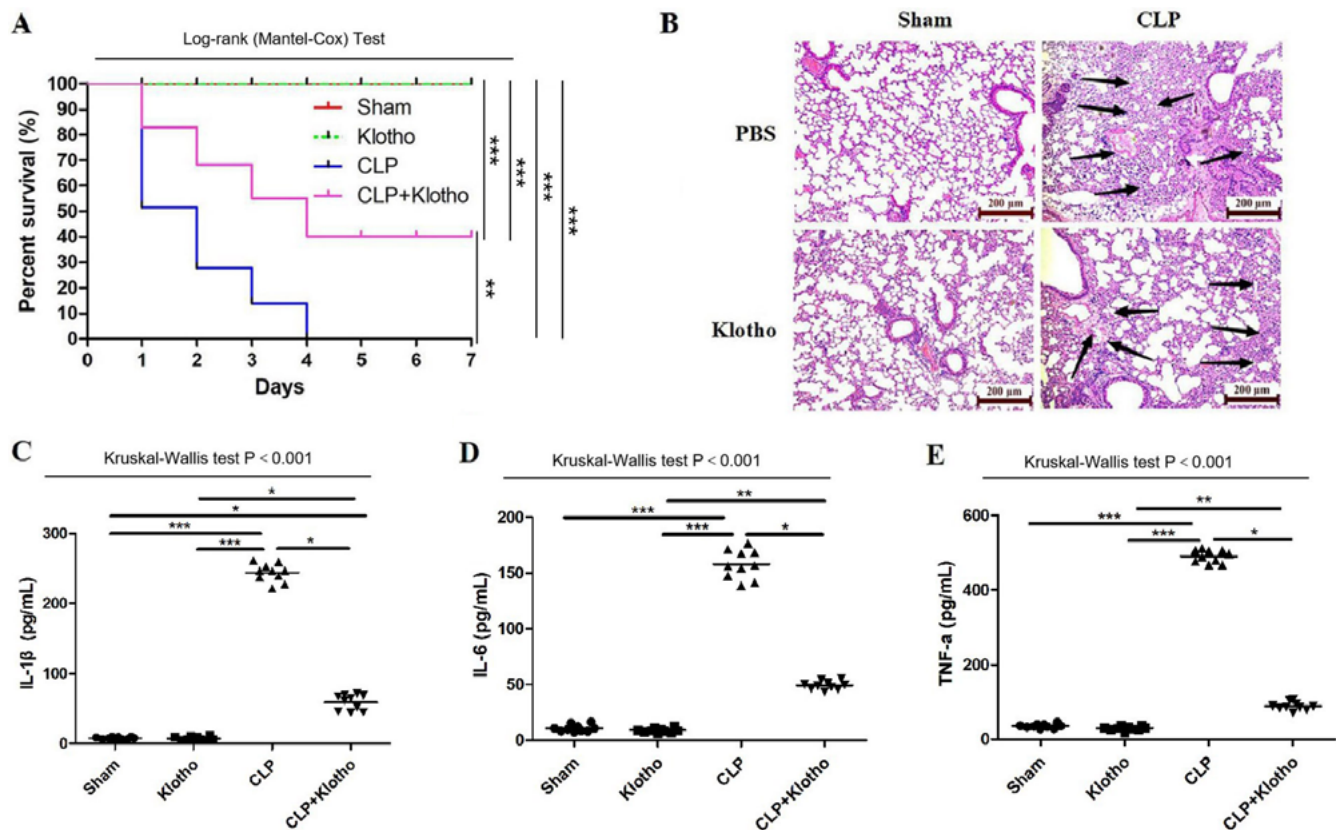


Fig. 1. Klotho increased the survival of mice with sepsis and decreased the release of interleukin (IL)-1 β , IL-6 and tumor necrosis factor alpha (TNF- α). A. The survival rates of mice in the sham, Klotho, cecal ligation and puncture (CLP), and Klotho+CLP groups ($n = 20$ /group) were analyzed. Data were analyzed with the log-rank (Mantel-Cox) test; ** $p < 0.002$ compared with the CLP group; *** $p < 0.001$ compared with the CLP group or CLP+Klotho group. B. Hematoxylin and eosin (H&E) staining was performed to detect the morphological structure of the lung tissue of mice in the 4 groups ($n = 10$ /group). C–E. IL-1 β , IL-6, and TNF- α levels were measured ($n = 10$ /group). The graph presents the results of data dots and medians. Data were analyzed with the Kruskal–Wallis test, and then Dunn's multiple comparison test was used for post hoc analysis; *** $p < 0.001$ compared with the CLP group; * $p < 0.05$ and ** $p < 0.01$ compared with the CLP+Klotho group

Lipopolysaccharide-induced apoptosis, inflammatory factor release and Bcl-2/Bax/caspase-3 pathway activation in HPAEpiCs

Human pulmonary alveolar epithelial cells were exposed to 0.1 mg/L, 1 mg/L or 10 mg/L LPS for 24 h or 10 mg/L LPS for 12 h, 24 h and 48 h, followed by cell viability assessment. The results showed that LPS reduced cell viability in a concentration- ($p < 0.05$; Fig. 3A) and time-dependent manner ($p < 0.05$; Fig. 3B). The apoptotic rate of HPAEpiCs was tested using Annexin/PI staining. Lipopolysaccharide significantly increased the percentage of apoptotic cells compared with that in the control group ($p < 0.05$; Fig. 3C–D). In addition, 10 mg/L LPS significantly increased the release of IL-1 β ($p < 0.05$), IL-6 ($p < 0.05$) and TNF- α ($p < 0.05$; Fig. 3E–G).

Because LPS induced HPAEpiC apoptosis, we detected the protein expression of Bcl-2, Bax and cleaved caspase-3 in LPS-treated cells. The results illustrated that LPS decreased the Bcl-2/GAPDH ratio ($p < 0.01$) and increased the Bax/GAPDH and cleaved caspase-3/pro-caspase-3 ratios (both $p < 0.05$; Fig. 3H–K). These results indicated that LPS induced apoptosis and Bcl-2/Bax/caspase-3 pathway activation in HPAEpiCs.

Effect of recombinant Klotho protein on viability, apoptosis and inflammatory factor release in LPS-exposed HPAEpiCs

To explore the effect of Klotho protein on the viability of LPS-exposed HPAEpiCs, we treated HPAEpiCs with LPS (10 mg/L) for 1 h followed by incubation with 10 mg/L, 50 mg/L or 100 mg/L recombinant Klotho for 24 h or 50 mg/L recombinant Klotho protein for 12 h, 24 h or 48 h. The results indicated that recombinant Klotho protein reversed the LPS-induced decrease in cell viability in a concentration- ($p < 0.05$; Fig. 4A) and time-dependent manner ($p < 0.001$; Fig. 4B). The apoptotic rate of HPAEpiCs was tested using Annexin/PI staining (Fig. 4C). As previously observed, 10 mg/L LPS induced significant apoptosis in HPAEpiCs ($p < 0.01$), and this effect was reversed by 50 mg/L recombinant Klotho protein treatment ($p < 0.05$; Fig. 4D). In addition, recombinant Klotho protein treatment reversed the LPS-induced release of IL-1 β , IL-6 and TNF- α (all $p < 0.05$; Fig. 4E–G).

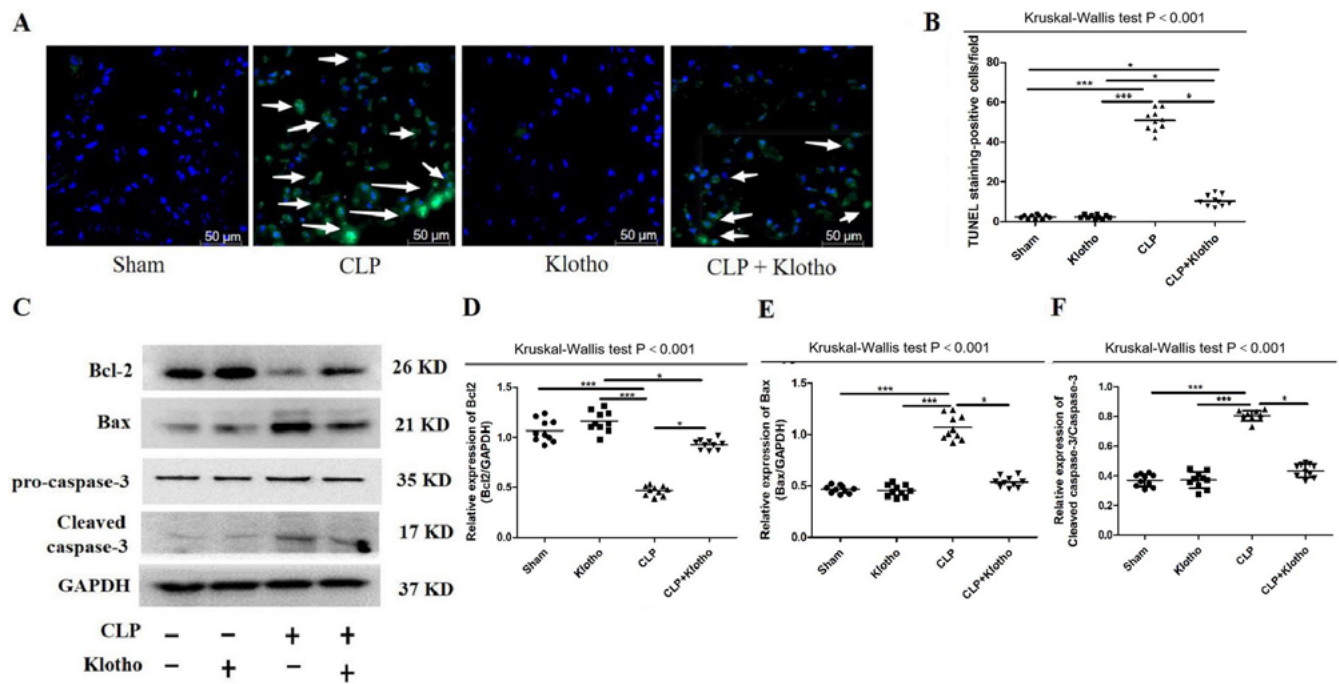


Fig. 2. Effects of Klotho on alveolar epithelial cell apoptosis and Bcl-2/Bax/caspase-3 signaling in mice with sepsis. A,B. The terminal deoxynucleotidyl transferase-mediated biotinylated UTP labeling (TUNEL) assay was performed to detect apoptotic cells in the lung tissues of mice in the sham, cecal ligation and puncture (CLP), Klotho, and CLP+Klotho groups ($n = 10/\text{group}$). TUNEL-positive cells were counted and compared among the groups. The graph presents the results of data dots and medians. The data were analyzed with the Kruskal–Wallis test, and then Dunn’s multiple comparison test was used for post hoc analysis; $*p < 0.05$ and $***p < 0.001$ compared with the CLP group. C–F. Western blotting was performed to detect the expression of Bcl-2, Bax, pro-caspase-3, and cleaved caspase-3. The graph presents the results of data dots and medians. The data were analyzed with the Kruskal–Wallis test, and then the Dunn’s multiple comparison test was used for post hoc analysis; $*p < 0.05$ and $***p < 0.001$ compared with the CLP group.

Recombinant Klotho protein blocked Bcl-2/Bax/caspase-3 signaling in LPS-exposed HPAEpiCs

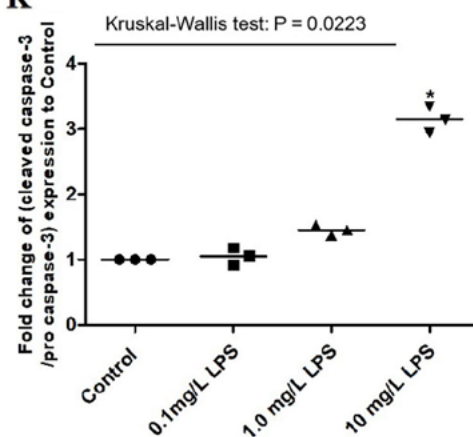
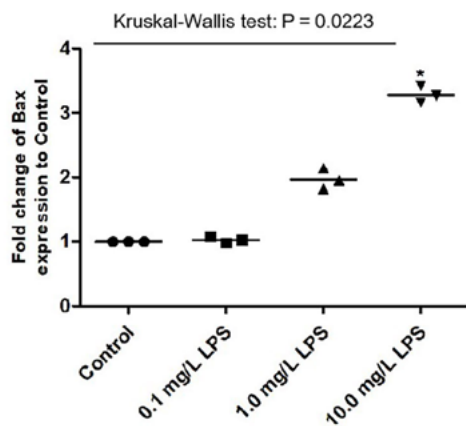
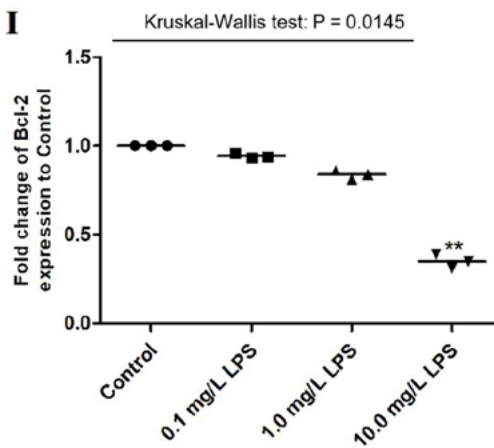
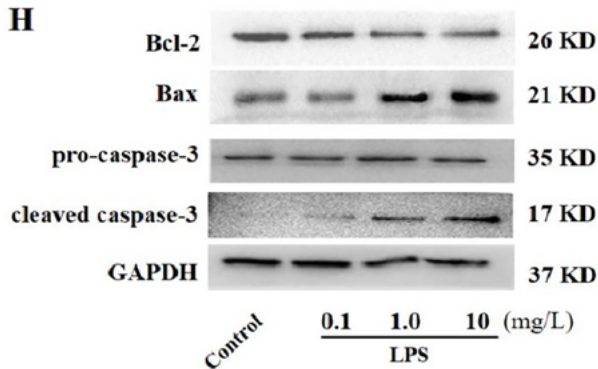
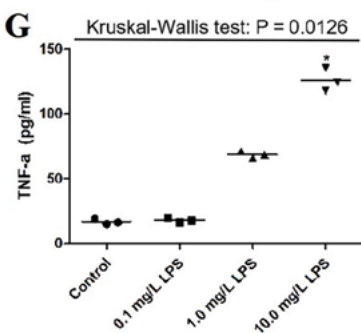
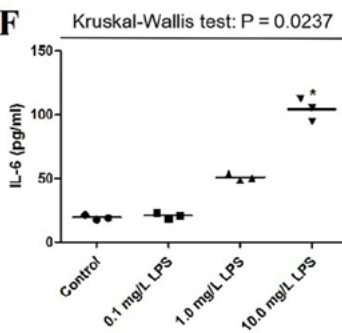
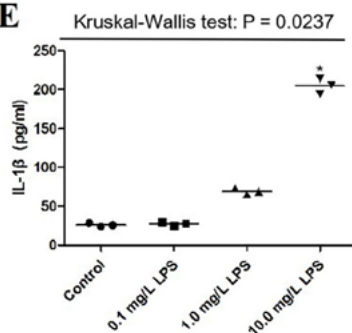
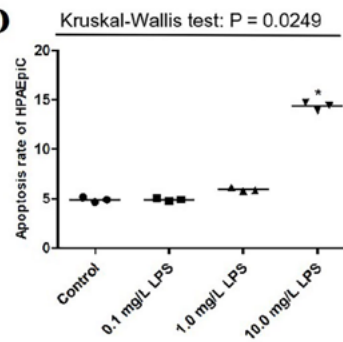
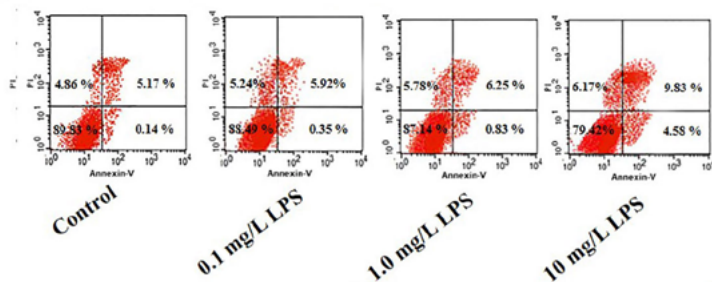
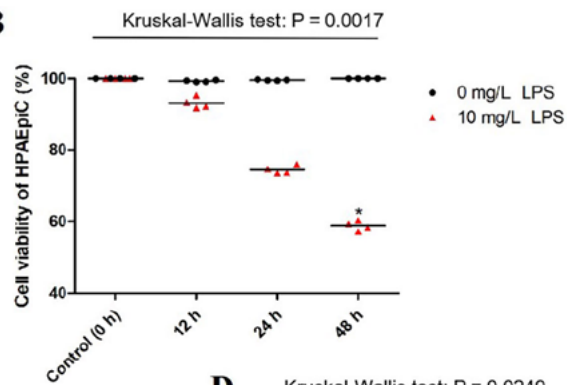
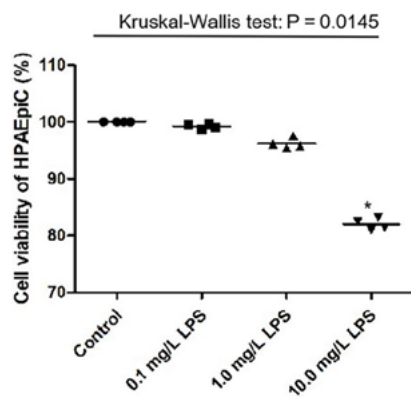
The cells were treated with LPS (10 mg/L) for 1 h and then incubated with 50 mg/L recombinant Klotho protein, after which we detected the protein expression of Bcl-2, Bax, pro-caspase-3, and cleaved caspase-3. The results demonstrated that LPS decreased the Bcl-2/GAPDH ratio and increased the Bax/GAPDH and cleaved caspase-3/pro-caspase-3 ratios (all $p < 0.01$), and these effects were partially reversed by recombinant Klotho protein administration (all $p < 0.05$; Fig. 5A–D).

Discussion

In vivo, we found that recombinant Klotho protein significantly reduced the inflammatory response and percentage of apoptotic cells in lung tissue, increased the survival rate of mice with sepsis and prevented the activation of BCL-2/Bax/caspase-3 signaling. Moreover, we observed that Klotho increased the viability and decreased the apoptosis of HPAEpiCs exposed to LPS in vitro. Finally, we demonstrated that LPS activated the Bcl-2/Bax/caspase-3 pathway, which was inhibited by Klotho.

The lungs represent the initial organ affected by inflammation in sepsis.³⁸ Sepsis causes severe systemic inflammatory response syndrome, leading to ARDS/

Fig. 3. Lipopolysaccharide induced apoptosis and activated the Bcl-2/Bax/caspase-3 pathway in human pulmonary alveolar epithelial cells (HPAEpiCs). A. Human pulmonary alveolar epithelial cells were exposed to 0.1 mg/L, 1 mg/L or 10 mg/L LPS for 24 h, and then the Cell Counting Kit-8 (CCK-8) assay was performed to detect cell viability. The graph presents the results of data dots and medians. Data were analyzed with the Kruskal–Wallis test. The Dunn’s multiple comparison test was used for post hoc analysis; $*p < 0.05$ compared with the control group. B. Human pulmonary alveolar epithelial cells were exposed to 10 mg/L LPS, and the CCK-8 assay was performed to detect cell viability after 12 h, 24 h and 48 h. The graph presents the results of data dots and medians. Data were analyzed with the Kruskal–Wallis test. A Dunn’s multiple comparison test was used for post hoc analysis; $*p < 0.05$ compared with the control (0 h) group. C–D. Human pulmonary alveolar epithelial cells were treated with LPS (0.1 mg/L, 1 mg/L or 10 mg/L) for 24 h, and the apoptosis rate was determined with flow cytometry. The graph presents the results of data dots and medians. Data were analyzed with the Kruskal–Wallis test. The Dunn’s multiple comparison test was used for post hoc analysis; $*p < 0.05$ compared with the control group. E–G. Interleukin (IL)-1 β , IL-6, and tumor necrosis factor alpha (TNF- α) levels were detected using enzyme-linked immunosorbent assay (ELISA). The graph presents the results of data dots and medians. Data were analyzed with the Kruskal–Wallis test. The Dunn’s multiple comparison test was used for post hoc analysis; $*p < 0.05$ compared with the control group. H. Human pulmonary alveolar epithelial cells were treated with 0.1 mg/L, 1 mg/L or 10 mg/L LPS for 24 h, and the expression of Bcl-2, Bax, pro-caspase-3, and cleaved caspase-3 was detected with western blotting. I–K. The graph presents the results of data dots and medians. Data were analyzed with the Kruskal–Wallis test. The Dunn’s multiple comparison test was used for post hoc analysis; $*p < 0.05$ and $**p < 0.01$ compared with the control group.



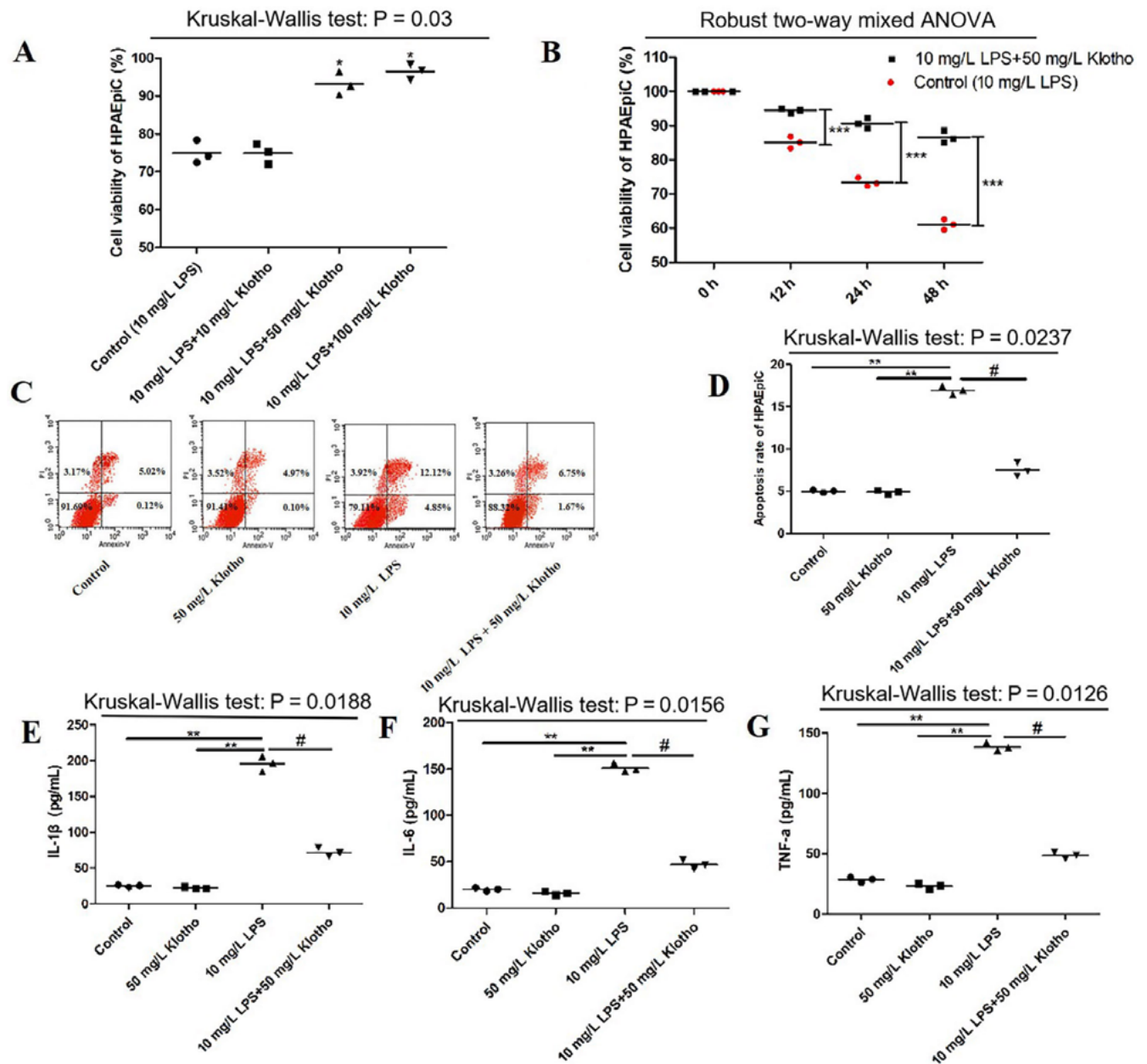


Fig. 4. Effects of recombinant Klotho protein on cell viability, apoptosis and inflammatory factor expression in lipopolysaccharide-treated human pulmonary alveolar epithelial cells. **A.** Human pulmonary alveolar epithelial cells were pretreated with 10 mg/L lipopolysaccharide (LPS) for 1 h and then incubated with various concentrations of recombinant Klotho (10 mg/L, 50 mg/L and 100 mg/L) for 24 h. The Cell Counting Kit-8 (CCK-8) assay was performed to detect cell viability. The graph presents the results of data dots and medians. Data were analyzed with the Kruskal–Wallis test. The Dunn’s multiple comparison test was used for post hoc analysis; $^{*}p < 0.05$ compared with the control group; **B.** Human pulmonary alveolar epithelial cells were pretreated with 10 mg/L LPS for 1 h, followed by treatment with 50 mg/L recombinant Klotho protein for different periods (12 h, 24 h and 48 h). Cell viability was assessed using the CCK-8 assay. The graph presents the results of data dots and medians. Data were analyzed with Robust 2-way mixed analysis of variance (ANOVA) using WRS2 package; $^{***}p < 0.001$ compared with the control group. **C, D.** Cells were pretreated with 10 mg/L LPS for 1 h followed by incubation with 50 mg/L recombinant Klotho protein for 24 h. The apoptosis rate was determined with flow cytometry. The graph presents the results of data dots and medians. Data were analyzed with the Kruskal–Wallis test. The Dunn’s multiple comparison test was used for post hoc analysis; $^{**}p < 0.01$ compared with the 10 mg/L LPS group; $^{*}p < 0.05$ compared with the 10 mg/L LPS+50 mg/L Klotho group; **E–G.** Interleukin (IL)-1 β , IL-6, and tumor necrosis factor alpha (TNF- α) levels in the cell culture medium were detected using enzyme-linked immunosorbent assay (ELISA). The graph presents the results of data dots and medians. Data were analyzed with the Kruskal–Wallis test. Dunn’s multiple comparison test was used for post hoc analysis; $^{***}p < 0.01$ compared with the 10 mg/L LPS group; $^{*}p < 0.05$ compared with the 10 mg/L LPS + 50 mg/L Klotho group

acute lung injury (ALI) and high mortality and morbidity rates.³⁹ In ARDS, severe inflammation caused by bacterial infection disrupts the endothelial barrier, increasing the permeability of the pulmonary vasculature to circulating fluids, macromolecules and leukocytes, and resulting in alveolar flooding and neutrophil influx,

which is responsible for the high mortality rate.⁴⁰ One of the pathophysiological characteristics of sepsis and subsequent ARDS/ALI are hyperactive and dysregulated endogenous inflammatory cytokines, such as IL-6, IL-1 β and TNF- α .^{41–44} In our study, we observed that CLP-induced sepsis decreased survival in mice and increased alveolar

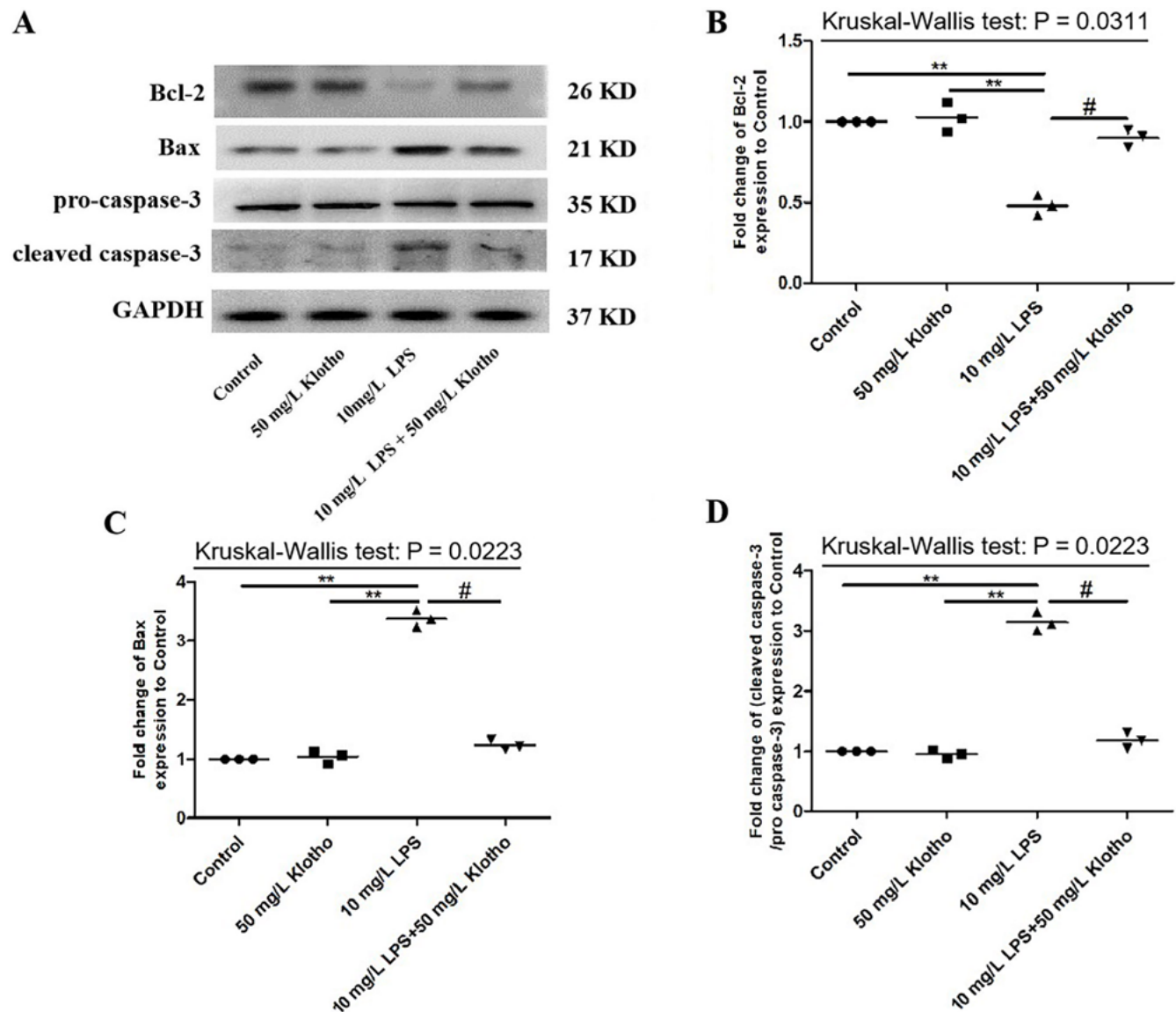


Fig. 5. Recombinant Klotho protein blocked the lipopolysaccharide (LPS)-induced activation of the Bcl-2/Bax/caspase-3 pathway in human pulmonary alveolar epithelial cells. A–D. Human pulmonary alveolar epithelial cells were pretreated with 10 mg/L LPS for 1 h and then incubated with 50 mg/L recombinant Klotho protein for 24 h. Bcl-2, Bax, pro-caspase-3, and cleaved caspase-3 expression were detected with western blotting. The graph presents the results of data dots and medians. Data were analyzed with the Kruskal–Wallis test. The Dunn’s multiple comparison test was used for post hoc analysis; ** $p < 0.01$ compared with the 10 mg/L LPS group; # $p < 0.05$ compared with the 10 mg/L LPS + 50 mg/L Klotho group

flooding, neutrophil influx and inflammatory factor release in the lungs. Human pulmonary alveolar epithelial cells apoptosis contributes to the pathogenesis of ALI and ARDS, which are common complications of sepsis.^{45,46} Upon apoptosis in alveolar epithelial cells, DNA breaks are induced, and the cell decreases in size, resulting in its destruction by nearby phagocytes. These events lead to the destruction of the alveolar epithelium and serious damage to the alveolar–capillary barrier, which in turn promotes the pathogenesis of ALI and ARDS.⁴⁷ Our study found that CLP induced apoptosis in alveolar epithelial cells in mouse lung tissue.

Sepsis is mostly caused by endotoxin, which is released from Gram-negative bacteria.⁴⁸ Lipopolysaccharide is an important component of endotoxin that can cause a cascade of immune stimulation and toxic

pathophysiological activities in the body, including ALI induced by sepsis.⁴⁹ Lipopolysaccharide is often used to generate animal models of diseases involving dysregulated inflammatory responses, such as ALI.^{50,51} Accumulating evidence indicates that inflammation is involved in apoptosis,⁵² and it has been reported that LPS can induce apoptosis in neurons,⁵³ cardiomyocytes,⁵⁴ renal tubular cells,⁵⁵ macrophages,⁵⁶ and HPAEpiCs.⁵⁷ Our research also found that LPS decreased the viability and increased the apoptosis rate in HPAEpiCs.

An imbalance between Bax and Bcl-2 plays an important role in the mitochondria-mediated caspase cascade, which was confirmed by an increased Bax/Bcl-2 ratio, release of cytochrome C from the mitochondria to the cytoplasm, cleavage of caspase-3, and subsequent induction of apoptosis.^{58,59} Yang et al. reported that LPS induced apoptosis

in alveolar macrophage cells by increasing the Bax/Bcl-2 ratio,⁶⁰ while Chopra et al. demonstrated that CLP-induced sepsis resulted in myocardial apoptosis through upregulation of the ratio of Bax/Bcl-2.⁶¹ Herein, we demonstrated that CLP and LPS treatment resulted in decreased Bcl-2 expression and increased Bax and cleaved caspase-3 expression.

Klotho is expressed primarily in renal cells, and it has anti-sepsis properties.²⁰ It has been reported that renal Klotho expression was significantly reduced in patients with sepsis-induced acute kidney injury (AKI) and in mice with sepsis.⁶² Recombinant Klotho ameliorates sepsis-induced multiple organ dysfunction,^{63–65} whereas Klotho deficiency has been reported to increase the production of TNF- α , IL-1 β and IL-6, which aggravate sepsis-induced multiple organ dysfunction syndrome.²⁰ In a CLP model, Klotho knockout mice exhibited significantly higher mortality, higher bacterial loads, and higher TNF- α , IL-6 and IL-10 concentrations.⁶⁶ In our study, Klotho increased the survival of mice with sepsis and decreased alveolar flooding, neutrophil influx and inflammatory factor release in the lungs of mice.

Accumulating evidence indicates that Klotho exerts anti-apoptotic effects; it has been shown to suppress endothelial apoptosis via a mitogen-activated kinase pathway.⁶⁷ Genetic Klotho deficiency increases cardiomyocyte apoptotic activity, whereas Klotho supplementation can reverse changes in apoptotic activity caused by D-galactose.⁶⁸ Klotho pretreatment inhibited apoptosis in retinal pigment epithelial cells by increasing Bcl-2 levels and decreasing Bax and cleaved caspase-3 levels. Moreover, it has been reported that Klotho protects lung epithelial cells from hyperoxia-induced apoptosis.⁶⁹ However, the effect of Klotho on CLP- or LPS-induced apoptosis in alveolar type II epithelial cells has never been explored. Our study has provided the first evidence that recombinant Klotho protein inhibited CLP- and LPS-induced apoptosis in HPAEpiCs. We also found that recombinant Klotho protein blocked the CLP- and LPS-induced activation of the Bcl-2/Bax/caspase-3 pathway in HPAEpiCs.

Limitations

We did not perform gene intervention in mouse lung tissue and HPAEpiCs. We also did not further explore the effect of Klotho on the Bcl-2/Bax/caspase-3 pathway, which are future research goals.

Conclusions

Our research indicated that recombinant Klotho protein protected alveolar type II epithelial cells against sepsis-induced apoptosis and increased their survival by blocking the Bcl-2/Bax/caspase-3 pathway. Considering the protective effect of Klotho on sepsis-induced apoptosis in alveolar

type II epithelial cells, it could represent a promising agent for treating sepsis-induced ALI.

Supplementary data

The Supplementary materials are available at <https://doi.org/10.5281/zenodo.10975284>. The package includes the following files:

Supplementary Table 1. Statistical methods, results and sample size for Fig. 1.

Supplementary Table 2. Statistical methods, results and sample size for Fig. 2.

Supplementary Table 3. Statistical methods, results and sample size for Fig. 3.

Supplementary Table 4. Statistical methods, results and sample size for Fig. 4.

Supplementary Table 5. Statistical methods, results and sample size for Fig. 5.

Data availability


The datasets generated and/or analyzed during the current study are available from the corresponding author on reasonable request.

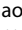
Consent for publication


Not applicable.


ORCID iDs

Xiao Bo Li  <https://orcid.org/0009-0009-1279-8842>

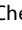
Jia Li Liu  <https://orcid.org/0009-0004-0386-4282>

Shuang Zhao  <https://orcid.org/0009-0006-7118-8364>

Jing Li  <https://orcid.org/0009-0002-5640-6651>

Guang-Yan Zhang  <https://orcid.org/0009-0002-2730-5800>

Qing Tang  <https://orcid.org/0009-0006-1684-6555>

Wei Yong Chen  <https://orcid.org/0009-0009-7296-3950>

References

1. Bringué J, Guillaumat-Prats R, Martinez M, et al. Methotrexate ameliorates systemic inflammation and septic associated-lung damage in a cecal ligation and puncture septic rat model. *Int J Mol Sci.* 2021; 22(17):9612. doi:10.3390/ijms22179612
2. Dushianthan A, Grocott MPW, Postle AD, Cusack R. Acute respiratory distress syndrome and acute lung injury. *Postgrad Med J.* 2011; 87(1031):612–622. doi:10.1136/pgmj.2011.118398
3. Beitler JR, Thompson BT, Baron RM, et al. Advancing precision medicine for acute respiratory distress syndrome. *Lancet Respir Med.* 2022; 10(1):107–120. doi:10.1016/S2213-2600(21)00157-0
4. Huppert L, Matthay M, Ware L. Pathogenesis of acute respiratory distress syndrome. *Semin Respir Crit Care Med.* 2019;40(1):031–039. doi:10.1055/s-0039-1683996
5. Ervin JN, Rentes VC, Dibble ER, et al. Evidence-based practices for acute respiratory failure and acute respiratory distress syndrome. *Chest.* 2020;158(6):2381–2393. doi:10.1016/j.chest.2020.06.080
6. Chesley CF, Anesi GL, Chowdhury M, et al. Characterizing equity of intensive care unit admissions for sepsis and acute respiratory failure. *Ann Am Thorac Soc.* 2022;19(12):2044–2052. doi:10.1513/AnnalsATS.202202-115OC
7. Drescher GS, Al-Ahmad MM. Analysis of noninvasive ventilation in subjects with sepsis and acute respiratory failure. *Respir Care.* 2021; 66(7):1063–1073. doi:10.4187/respcare.08599

8. Remick DG. Pathophysiology of sepsis. *Am J Pathol.* 2007;170(5): 1435–1444. doi:10.2353/ajpath.2007.060872
9. Erlanson-Albertsson C, Stenkula KG. The importance of food for endotoxemia and an inflammatory response. *Int J Mol Sci.* 2021;22(17):9562. doi:10.3390/ijms22179562
10. Tirunavalli SK, Gourishetti K, Kotipalli RSS, et al. Dehydrozingerone ameliorates lipopolysaccharide induced acute respiratory distress syndrome by inhibiting cytokine storm, oxidative stress via modulating the MAPK/NF- κ B pathway. *Phytomedicine.* 2021;92:153729. doi:10.1016/j.phymed.2021.153729
11. Carnino JM, Lee H, He X, Groot M, Jin Y. Extracellular vesicle-cargo miR-185-5p reflects type II alveolar cell death after oxidative stress. *Cell Death Discov.* 2020;6(1):82. doi:10.1038/s41420-020-00317-8
12. Tompkins KD, Thorburn A. Regulation of apoptosis by autophagy to enhance cancer therapy. *Yale J Biol Med.* 2019;92(4):707–718. PMID:31866785. PMCID:PMC6913805.
13. El Hayek MS, Ernande L, Benitah JP, Gomez AM, Pereira L. The role of hyperglycaemia in the development of diabetic cardiomyopathy. *Arch Cardiovasc Dis.* 2021;114(11):748–760. doi:10.1016/j.acvd.2021.08.004
14. Hoshyar R, Mollaei H. A comprehensive review on anticancer mechanisms of the main carotenoid of saffron, crocin. *J Pharm Pharmacol.* 2017;69(11):1419–1427. doi:10.1111/jphp.12776
15. Han JH, Park MH, Myung CS. *Garcinia cambogia* ameliorates non-alcoholic fatty liver disease by inhibiting oxidative stress-mediated steatosis and apoptosis through NRF2-ARE activation. *Antioxidants.* 2021;10(8):1226. doi:10.3390/antiox10081226
16. Du J, Song D, Cao T, et al. Saikosaponin-A induces apoptosis of cervical cancer through mitochondria- and endoplasmic reticulum stress-dependent pathway in vitro and in vivo: Involvement of PI3K/AKT signaling pathway. *Cell Cycle.* 2021;20(21):2221–2232. doi:10.1080/15384101.2021.1974791
17. Zhao S, Gao J, Li J, Wang S, Yuan C, Liu Q. PD-L1 regulates inflammation in LPS-induced lung epithelial cells and vascular endothelial cells by interacting with the HIF-1 α signaling pathway. *Inflammation.* 2021;44(5):1969–1981. doi:10.1007/s10753-021-01474-3
18. Hou L, Zhang J, Liu Y, et al. MitoQ alleviates LPS-mediated acute lung injury through regulating Nrf2/Drp1 pathway. *Free Radic Biol Med.* 2021;165:219–228. doi:10.1016/j.freeradbiomed.2021.01.045
19. Dounousi E, Torino C, Pizzini P, et al. Intact FGF23 and α -Klotho during acute inflammation/sepsis in CKD patients. *Eur J Clin Invest.* 2016; 46(3):234–241. doi:10.1111/eci.12588
20. Jorge LB, Coelho FO, Sanches TR, et al. Klotho deficiency aggravates sepsis-related multiple organ dysfunction. *Am J Physiol Renal Physiol.* 2019;316(3):F438–F448. doi:10.1152/ajprenal.00625.2017
21. Buchanan S, Combet E, Stenvinkel P, Shiels PG. Klotho, aging, and the failing kidney. *Front Endocrinol (Lausanne).* 2020;11:560. doi:10.3389/fendo.2020.00560
22. Lian WY, Lu ZP, Zhao W, et al. The role of Klotho protein against sevoflurane-induced neuronal injury. *Neurochem Res.* 2022;47(2):315–326. doi:10.1007/s11064-021-03444-5
23. Marquez-Exposito L, Tejedor-Santamaria L, Santos-Sanchez L, et al. Acute kidney injury is aggravated in aged mice by the exacerbation of proinflammatory processes. *Front Pharmacol.* 2021;12:662020. doi:10.3389/fphar.2021.662020
24. Xue M, Yang F, Le Y, et al. Klotho protects against diabetic kidney disease via AMPK- and ERK-mediated autophagy. *Acta Diabetol.* 2021; 58(10):1413–1423. doi:10.1007/s00592-021-01736-4
25. Zhuang X, Sun X, Zhou H, et al. Klotho attenuated doxorubicin-induced cardiomyopathy by alleviating dynamin-related protein 1-mediated mitochondrial dysfunction. *Mech Ageing Dev.* 2021;195:111442. doi:10.1016/j.mad.2021.111442
26. Xing L, Guo H, Meng S, et al. Klotho ameliorates diabetic nephropathy by activating Nrf2 signaling pathway in podocytes. *Biochem Biophys Res Commun.* 2021;534:450–456. doi:10.1016/j.bbrc.2020.11.061
27. Xu Z, Zheng S, Feng X, Cai C, Ye X, Liu P. Klotho gene improves oxidative stress injury after myocardial infarction. *Exp Ther Med.* 2020; 21(1):52. doi:10.3892/etm.2020.9484
28. Gagan JM, Cao K, Zhang YA, et al. Constitutive transgenic α -Klotho overexpression enhances resilience to and recovery from murine acute lung injury. *Am J Physiol Lung Cell Mol Physiol.* 2021;321(4):L736–L749. doi:10.1152/ajplung.00629.2020
29. Chen B, Wang X, Zhao W, Wu J. Klotho inhibits growth and promotes apoptosis in human lung cancer cell line A549. *J Exp Clin Cancer Res.* 2010;29(1):99. doi:10.1186/1756-9966-29-99
30. Xie J, Zhao ZZ, Li P, et al. Senkyunolide I protects against sepsis-associated encephalopathy by attenuating sleep deprivation in a murine model of cecal ligation and puncture. *Oxid Med Cell Longev.* 2021;2021:6647258. doi:10.1155/2021/6647258
31. Alves GF, Aimaretti E, Einaudi G, et al. Pharmacological inhibition of FAK-Pyk2 pathway protects against organ damage and prolongs the survival of septic mice. *Front Immunol.* 2022;13:837180. doi:10.3389/fimmu.2022.837180
32. Zhang W, Li L, Zheng Y, et al. *Schistosoma japonicum* peptide SJMHE1 suppresses airway inflammation of allergic asthma in mice. *J Cell Mol Med.* 2019;23(11):7819–7829. doi:10.1111/jcmm.14661
33. Yang H, Lv H, Li H, Ci X, Peng L. Oridonin protects LPS-induced acute lung injury by modulating Nrf2-mediated oxidative stress and Nrf2-independent NLRP3 and NF- κ B pathways. *Cell Commun Signal.* 2019; 17(1):62. doi:10.1186/s12964-019-0366-y
34. Resnick-Silverman L. Using TUNEL assay to quantitate p53-induced apoptosis in mouse tissues. *Methods Mol Biol.* 2021;2267:181–190. doi:10.1007/978-1-0716-1217-0_12
35. Wang L, Li S, Luo H, Lu Q, Yu S. PCSK9 promotes the progression and metastasis of colon cancer cells through regulation of EMT and PI3K/AKT signaling in tumor cells and phenotypic polarization of macrophages. *J Exp Clin Cancer Res.* 2022;41(1):303. doi:10.1186/s13046-022-02477-0
36. Zheng JY, Wang SC, Tang SC, et al. Sodium acetate ameliorates cisplatin-induced kidney injury in vitro and in vivo. *Chem Biol Interact.* 2023;369:110258. doi:10.1016/j.cbi.2022.110258
37. Di Silverio F, Gallucci M, Alpi G, et al. Indications and limits of percutaneous nephrolithotripsy and extracorporeal shock wave lithotripsy combined treatment. *Contrib Nephrol.* 1987;58:262–265. doi:10.1159/000414530
38. Sun R, Zhao N, Wang Y, et al. High concentration of hydrogen gas alleviates lipopolysaccharide-induced lung injury via activating Nrf2 signaling pathway in mice. *Int Immunopharmacol.* 2021;101:108198. doi:10.1016/j.intimp.2021.108198
39. Chen DQ, Shen MJ, Wang H, et al. Sirt3 maintains microvascular endothelial adherens junction integrity to alleviate sepsis-induced lung inflammation by modulating the interaction of VE-cadherin and β -catenin. *Oxid Med Cell Longev.* 2021;2021:8978795. doi:10.1155/2021/8978795
40. Matthay MA, Ware LB, Zimmerman GA. The acute respiratory distress syndrome. *J Clin Invest.* 2012;122(8):2731–2740. doi:10.1172/JCI60331
41. Bateman RM, Sharpe MD, Jagger JE, et al; South Yorkshire Hospitals Research Collaboration. 36th International Symposium on Intensive Care and Emergency Medicine: Brussels, Belgium. 15–18 March 2016. *Crit Care.* 2016;20(Suppl 2):94. doi:10.1186/s13054-016-1208-6
42. Montoya-Ruiz C, Jaimes FA, Rugeles MT, López JA, Bedoya G, Velilla PA. Variants in LTA, TNF, IL1B and IL10 genes associated with the clinical course of sepsis. *Immunol Res.* 2016;64(5–6):1168–1178. doi:10.1007/s12026-016-8860-4
43. Edelman DA, Jiang Y, Tyburski JG, Wilson RF, Steffes CP. Cytokine production in lipopolysaccharide-exposed rat lung pericytes. *J Trauma.* 2007;62(1):89–93. doi:10.1097/TA.0b013e31802dd712
44. Wang F, Fang B, Qiang X, Shao J, Zhou L. The efficacy of mesenchymal stromal cell-derived therapies for acute respiratory distress syndrome: A meta-analysis of preclinical trials. *Respir Res.* 2020;21(1):307. doi:10.1186/s12931-020-01574-y
45. Gong Y, Lan H, Yu Z, et al. Blockage of glycolysis by targeting PFKFB3 alleviates sepsis-related acute lung injury via suppressing inflammation and apoptosis of alveolar epithelial cells. *Biochem Biophys Res Commun.* 2017;491(2):522–529. doi:10.1016/j.bbrc.2017.05.173
46. Kimura H, Suzuki M, Konno S, et al. Orchestrating role of apoptosis inhibitor of macrophage in the resolution of acute lung injury. *J Immunol.* 2017;199(11):3870–3882. doi:10.4049/jimmunol.1601798
47. Gu LZ, Sun H. Lonicerin prevents inflammation and apoptosis in LPS-induced acute lung injury. *Front Biosci.* 2020;25(3):480–497. doi:10.2741/4815
48. Wohlfart S, Kilian M, Storck P, Gutschmann T, Brandenburg K, Mier W. Mass spectrometric quantification of the antimicrobial peptide Pep19-2.5 with stable isotope labeling and acidic hydrolysis. *Pharmaceutics.* 2021;13(9):1342. doi:10.3390/pharmaceutics13091342

49. Wann S, Chi P, Huang W, Cheng C, Chang Y. Combination therapy of iPSC-derived conditioned medium with ceftriaxone alleviates bacteria-induced lung injury by targeting the NLRP3 inflammasome. *J Cell Physiol.* 2022;237(2):1299–1314. doi:10.1002/jcp.30596
50. Su VYF, Chen WC, Yu WK, Wu HH, Chen H, Yang KY. Nintedanib regulates GRK2 and CXCR2 to reduce neutrophil recruitment in endotoxin-induced lung injury. *Int J Mol Sci.* 2021;22(18):9898. doi:10.3390/ijms22189898
51. Hong J, Mo S, Gong F, et al. lncRNA-SNHG14 plays a role in acute lung injury induced by lipopolysaccharide through regulating autophagy via miR-223-3p/Foxo3a. *Mediators Inflamm.* 2021;2021:7890288. doi:10.1155/2021/7890288
52. Wu X, Liu Y, Guo X, et al. Prolactin inhibits the progression of intervertebral disc degeneration through inactivation of the NF- κ B pathway in rats. *Cell Death Dis.* 2018;9(2):98. doi:10.1038/s41419-017-0151-z
53. Liu J, Lin M, Qiao F, Zhang C. Exosomes derived from lncRNA TCTN2-modified mesenchymal stem cells improve spinal cord injury by miR-329-3p/IGF1R axis. *J Mol Neurosci.* 2022;72(3):482–495. doi:10.1007/s12031-021-01914-7
54. Luo Y, Tu H, Yang Z, et al. Long non-coding RNA MALAT1 silencing elevates microRNA-26a-5p to ameliorate myocardial injury in sepsis by reducing regulator of calcineurin 2. *Arch Biochem Biophys.* 2022;715:109047. doi:10.1016/j.abb.2021.109047
55. Gao Z, Lu L, Chen X. Release of HMGB1 in podocytes exacerbates lipopolysaccharide-induced acute kidney injury. *Mediators Inflamm.* 2021;2021:5220226. doi:10.1155/2021/5220226
56. Zhang S, Fu B, Xiong Y, et al. Tgm2 alleviates LPS-induced apoptosis by inhibiting JNK/BCL-2 signaling pathway through interacting with Aga in macrophages. *Int Immunopharmacol.* 2021;101:108178. doi:10.1016/j.intimp.2021.108178
57. Nan CC, Zhang N, Cheung KCP, et al. Knockdown of lncRNA MALAT1 alleviates LPS-induced acute lung injury via inhibiting apoptosis through the miR-194-5p/FOXP2 axis. *Front Cell Dev Biol.* 2020;8:586869. doi:10.3389/fcell.2020.586869
58. Li J, Liu F, Jiang S, et al. Berberine hydrochloride inhibits cell proliferation and promotes apoptosis of non-small cell lung cancer via the suppression of the MMP2 and Bcl-2/Bax signaling pathways. *Oncol Lett.* 2018;15(5):7409–7414. doi:10.3892/ol.2018.8249
59. Strasser A, O'Connor L, Dixit VM. Apoptosis signaling. *Annu Rev Biochem.* 2000;69(1):217–245. doi:10.1146/annurev.biochem.69.1.217
60. Yang L, Zhang Z, Zhuo Y, et al. Resveratrol alleviates sepsis-induced acute lung injury by suppressing inflammation and apoptosis of alveolar macrophage cells. *Am J Transl Res.* 2018;10(7):1961–1975. PMID:30093935. PMCID:PMC6079135.
61. Chopra M, Sharma AC. Distinct cardiodynamic and molecular characteristics during early and late stages of sepsis-induced myocardial dysfunction. *Life Sci.* 2007;81(4):306–316. doi:10.1016/j.lfs.2007.05.021
62. Jou-Valencia D, Molema G, Popa E, et al. Renal Klotho is reduced in septic patients and pretreatment with recombinant Klotho attenuates organ injury in lipopolysaccharide-challenged mice. *Crit Care Med.* 2018;46(12):e1196–e1203. doi:10.1097/CCM.00000000000003427
63. Liu X, Niu Y, Zhang X, et al. Recombinant α -Klotho protein alleviated acute cardiorenal injury in a mouse model of lipopolysaccharide-induced septic cardiorenal syndrome type 5. *Anal Cell Pathol (Amst).* 2019;2019:5853426. doi:10.1155/2019/5853426
64. Chen X, Tong H, Chen Y, et al. Klotho ameliorates sepsis-induced acute kidney injury but is irrelevant to autophagy. *Onco Targets Ther.* 2018;11:867–881. doi:10.2147/OTT.S156891
65. C ndor JM, Rodrigues CE, De Sousa Moreira R, et al. Treatment with human Wharton's jelly-derived mesenchymal stem cells attenuates sepsis-induced kidney injury, liver injury, and endothelial dysfunction. *Stem Cell Transl Med.* 2016;5(8):1048–1057. doi:10.5966/sctm.2015-0138
66. Abdelmalik PA, Stevens RD, Singh S, et al. Anti-aging factor, serum α -Klotho, as a marker of acute physiological stress, and a predictor of ICU mortality, in patients with septic shock. *J Crit Care.* 2018;44:323–330. doi:10.1016/j.jcrr.2017.11.023
67. Maekawa Y, Ohishi M, Ikushima M, et al. Klotho protein diminishes endothelial apoptosis and senescence via a mitogen-activated kinase pathway. *Geriatr Gerontol Int.* 2011;11(4):510–516. doi:10.1111/j.1447-0594.2011.00699.x
68. Li-Zhen L, Chen Z, Wang SS, Liu W, Zhuang X. Klotho deficiency causes cardiac ageing by impairing autophagic and activating apoptotic activity. *Eur J Pharmacol.* 2021;911:174559. doi:10.1016/j.ejphar.2021.174559
69. Kim SJ, Chereshe P, Eren M, et al. Klotho, an antiaging molecule, attenuates oxidant-induced alveolar epithelial cell mtDNA damage and apoptosis. *Am J Physiol Lung Cell Mol Physiol.* 2017;313(1):L16–L26. doi:10.1152/ajplung.00063.2017